Hindawi
Shock and Vibration
Volume 2021, Article ID 8814962, 8 pages
https://doi.org/10.1155/2021/8814962

Research Article

Band Gap and Vibration Reduction Properties of Damped Rail with Two-Dimensional Honeycomb Phononic Crystals

Rixin Cui, Jinsong Zhou, and Dao Gong

Institute of Rail Transit, Tongji University, Shanghai 201804, China

Correspondence should be addressed to Jinsong Zhou; jinsong.zhou@tongji.edu.cn

Received 7 August 2020; Revised 31 December 2020; Accepted 25 January 2021; Published 9 February 2021

Academic Editor: Pedro A. Costa

Copyright © 2021 Rixin Cui et al. This is an open access article distributed under the Creative Commons Attribution License, which permits unrestricted use, distribution, and reproduction in any medium, provided the original work is properly cited.

The prevention of environmental vibration pollution induced by train operation is one of the inevitable problems in the construction of urban rail transit. With the advantage of flexible adjustment, phononic crystals (PCs) have a broad application prospect in suppressing elastic wave propagation of rail transit. In this paper, a damped rail with two-dimensional honeycomb PCs was proposed, and its band structure was analysed with FEM. Then, a parametric study was used to investigate the influences of design parameters of the honeycomb PCs on its band gap property. Furthermore, with a 3D half-track model, the vibration reduction property of the damped rail with honeycomb PCs was discussed. The results show that the damped rail with honeycomb PCs has an absolute band gap in the frequency range of 877.3–1501.7 Hz, which includes the pinned-pinned resonance frequency of the rail internally. Reducing the filling fraction and elastic modulus of the matrix can obtain an absolute band gap in a lower frequency range but also bring a narrower bandwidth. The decrease of scatterer density leads to higher boundary frequencies of the absolute band gap and descends the bandwidth. In order to obtain an absolute band gap which can suppress the pinned-pinned resonance of the rail and keep a wider bandwidth, the filling fraction is suitable to be about 0.5, and the elastic modulus of the matrix is proposed to be not more than 0.6 MPa. Metals with heavy density can be used as the scatterer to obtain a better vibration reduction effect. It is hoped that the research results can provide a reference for the application of PCs in track vibration reduction.

1. Introduction

Urban rail transit provides an efficient and low-cost way for residents to travel in the city. In recent years, the construction scale of urban rail transit has even become an indicator to estimate the prosperity of a city. However, as the density of urban rail transit network increases, the environmental vibration induced by train operation grows sharply, which has considerable effects on the safety of the protected ancient buildings, as well as the routine life and work of residents living along traffic-lines. The vibration reduction of urban rail transit has become an imperative problem in the construction of urban rail transit, which must be resolved promptly and properly.

The track vibration caused by the huge wheel/rail interaction force, which propagates along the foundation under track (subgrade, tunnel, or viaduct) and surrounding soil to adjacent buildings, is the fundamental source of environment vibration of urban rail transit. The essence of this process is the propagation of elastic waves in solid structures. Phononic crystals (PCs), composed of two or more different types of materials with different mechanical properties and mass densities, may exhibit band gaps, within which the propagation of elastic waves is prohibited [1]. As most of the PCs are artificial structures, they have flexible adjustment in the attenuation of elastic waves. Therefore, PCs may have potential applications in the control of noise or vibration in railway.

At present, the advantages of PCs in vibration and noise reduction have gradually attracted the attention of scholars in the field of rail transit, and some researches on the track vibration reduction with PCs have also been conducted. Considering the dynamic vibration absorbers (DVAs) as periodic devices installed on the rail, Xiao et al. discussed the influences of this passive vibration reduction method on the dispersion and vibration properties of the CRTS II slab track

[2]. Wang et al. attached locally resonant units on the rail periodically and explicated the formation mechanism of the new wider band gap of the track in high-speed railway [3]. The introduction of PCs into floating slab track (FST) system can improve its vibration isolation effect effectively. Based on the local resonance mechanism, Sheng et al. [4] and Nong et al. [5] designed vibration isolators with locally resonant PCs to replace the steel springs in the FST, respectively. The new FST using PCs can get an improvement in overall vibration mitigation performance with their band gap properties. Zhao et al. developed a kind of locally resonant damping pad composed of cubic steel scatterers sandwiched between two soft rubber coatings [6], and the test results proved that the new damping pad can get a better effect with a vibration reduction of 10 dB. Jiang et al. proposed a two-dimensional ternary locally resonant periodic row-pile structure with hexagonal lattice to prohibit the propagation of the environmental vibration in low-frequency range, and the vibration reduction effect is related to the soil property around the row-piles [7]. By adding 22% light polymer particles evenly into ordinary concrete, Miao et al. developed a composite track bed with two band gaps in the frequency of 0~30 Hz and 45~135 Hz, which can be used for low-frequency vibration reduction of ballastless tracks [8]. Yi et al. proposed an air-solid periodic noise barrier for rail transit on subgrade or viaduct [9], which can improve the noise reduction effect by 2~3 dB compared with the ordinary erect sound barrier of the same mass.

The damped rail is an effective control method for mitigating railway vibration and noise at the source [10]. Therefore, a kind of damped rail with two-dimensional honeycomb PCs is proposed in this paper, and its band structure is calculated with finite element method (FEM). Then, the influences of structural and material parameters of the honeycomb PCs on its band gap property are analysed. With a 3D half-track model, the vibration reduction effect of the damped rail with honeycomb PCs is discussed. It is hoped that the research results can provide a reference for the application of PCs in track vibration reduction.

1.1. Proposed Damped Rail with PCs. The proposed damped rail with two-dimensional honeycomb PCs is composed of hexagonal metal scatterers and the matrix made of vulcanized rubber, which can be bonded to the rail web, as shown in Figure 1(a). The scatterers are embedded in the rubber matrix with triangular lattice. The band gaps of the two-dimensional honeycomb PCs are generated based on the Bragg scattering mechanism. The unit cells and basic vectors in direct lattices are shown in Figure 1(b). The first Brillouin zone and irreducible Brillouin zone are shown in Figure 1(c).

Considering the limit of the geometric space of the rail web, the lattice constant a and side length of hexagonal metal scatterer e of the unit cell in damped rail with PCs can be given as follows: $a = 11.29$ mm; $e = 4.5$ mm. The material parameters of the matrix and the scatterer are listed in Table 1.

The damped rail with two-dimensional honeycomb PCs can not only control the rail vibration propagation through the band gap theory but also retain the energy dissipation principle of the traditional damped rail. When the hexagonal metal scatterers vibrate with the rail, the relative motion between adjacent scatterers will bring compression and shear to the matrix rubber, which can further dissipate the vibration energy through the damping deformation.

1.2. Band Gap Property. When an ideal elastic body deforms slightly, the governing equation of motion without the body force is expressed as [11]

$$\rho\ddot{\mathbf{u}}(\mathbf{r},t) = (\lambda+\mu)\nabla\nabla\cdot\mathbf{u}(\mathbf{r},t) + \mu\nabla^2\mathbf{u}(\mathbf{r},t), \tag{1}$$

where $\mathbf{u}(\mathbf{r},t)$ is the displacement function vector; $\mathbf{r}$ is the coordinate vector corresponding to x, y, z directions; t is the time; ρ is the density; λ and μ are the Lamé constants; and ∇ is the Hamilton differential operator.

In the case of two-dimensional systems, the scatterers are supposed to be parallel to z-axis with the wave vector lying in the xy-plane. Then, the terms of partial derivative of z in equation (1) are all zero, and u_z is independent. Therefore, equation (1) can be decoupled into two groups of equations of motion in xy-plane and z direction, which are called wave equation of in-plane (xy-) mode (equation (2)) and wave equation of antiplane (z-) mode (equation (3)), respectively,

$$\rho(\mathbf{r})\ddot{u}_{xy}(\mathbf{r},t) = (\lambda(\mathbf{r})+\mu(\mathbf{r}))\nabla\nabla\cdot\mathbf{u}_{xy}(\mathbf{r},t) + \mu(\mathbf{r})\nabla^2\mathbf{u}_{xy}(\mathbf{r},t), \tag{2}$$

$$\rho(\mathbf{r})\ddot{u}_z(\mathbf{r},t) = \mu(\mathbf{r})\nabla^2\mathbf{u}_z(\mathbf{r},t), \tag{3}$$

where $\rho(\mathbf{r})$, $\lambda(\mathbf{r})$, and $\mu(\mathbf{r})$ are periodic functions of coordinate vector $\mathbf{r}$.

The elastic wave in phononic crystal structure is a kind of Bloch wave. Thus, the solution of equation (1) satisfies the Bloch theorem [12]:

$$\mathbf{u}(\mathbf{r},t) = \mathbf{v}(\mathbf{r})e^{i(\mathbf{k}\cdot\mathbf{r}-wt)}, \tag{4}$$

where $\mathbf{k}$ is the wave vector of the reciprocal space; ω is the angular frequency; and $\mathbf{v}(\mathbf{r})$ is the wave amplitude. Considering the periodicity of the structure, $\mathbf{v}(\mathbf{r})$ can be expressed as

$$\mathbf{v}(\mathbf{r}+\mathbf{R_n}) = \mathbf{v}(\mathbf{r}), \tag{5}$$

where $\mathbf{R_n}$ is the periodic constant vector. The periodic boundary conditions can be obtained by substituting equation (5) into equation (4):

$$\mathbf{u}(\mathbf{r}+\mathbf{R_n},t) = \mathbf{u}(\mathbf{r},t)e^{i\mathbf{k}\cdot\mathbf{R_n}}. \tag{6}$$

As the two-dimensional honeycomb PCs attached to the damped rail are Bragg scattering PCs, the rubber matrix only acts as a mass block [13]. Therefore, the coupling between the matrix and the scatterer can be neglected during the calculation of the band structure. By applying equation (6) to the wave equations, the eigenvalue problem involving the relationship between wave frequency and wave vector can be obtained. Taking the wave vector along the boundaries of the irreducible

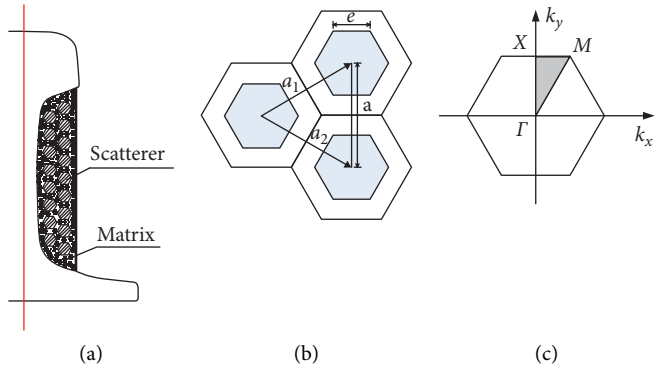

Figure 1: Damped rail with two-dimensional honeycomb PCs. (a) Schematic illustration. (b) Unit cells. (c) The first Brillouin zone.

Table 1: Material parameters of matrix and scatterer.

	Material	Density (kg/m^3)	Elastic modulus (N/m^2)	Poisson's ratio
Matrix	Vulcanized rubber	1300	5.00×10^5	0.470
Scatterer	Pb	11600	4.08×10^{10}	0.369

Brillouin zone (M-Γ-X-M) shown in Figure 1(c), the band structure of elastic waves in PCs can be solved.

At present, the calculation methods for band structure of PCs mainly include the transfer matrix method generally applied to one-dimensional PCs [14], plane wave expansion method commonly applied to two-dimensional PCs [15], multiple scattering theory [16], finite difference time domain method [17], and FEM [18, 19], among which the FEM has the best applicability for complex structures. The finite element model of the two-dimensional honeycomb PC is divided using quadrilateral elements, and the degree of freedom of the meshed model is 4256. The Floquet periodic boundary condition is applied to the finite element model to deal with the Bloch wave. The velocity of compression waves (in xy-mode) $c_L = \sqrt{((\lambda + 2\mu)/\rho)}$, and the velocity of shear waves (in z-mode) $c_T = \sqrt{(\mu/\rho)}$. The scanning range of wave vector k_x is set as $0 \sim 2\pi/3a$, and k_y is set as $0 \sim (2\sqrt{3}\pi)/3a$. The band structure can be obtained by solving the generalized eigenvalue problem including the dispersion relation of elastic wave in the given range of the wave vectors.

The band structure for xy-mode and z-mode of the damped rail with two-dimensional honeycomb PCs is shown in Figures 2 and 3, respectively. It can be seen from Figure 2 that within the concerned frequency range of rail vibration, the proposed PCs structure has a complete band gap in the frequency range of 877.3~1704.2 Hz for xy-mode. Besides, there are six directional band gaps along the X-M direction and a directional band gap in the frequency range of 2242.7~2742.7 Hz along the Γ-X direction. Among the directional band gaps along the X-M direction, the largest bandwidth is 494.5 Hz, which is in the frequency range of 1748.1~2242.7 Hz. Within the abovementioned band gaps, the propagation of plane compression waves in the proposed PCs structure will be inhibited.

In Figure 3, there are four complete band gaps for the z-mode of the proposed two-dimensional honeycomb PCs

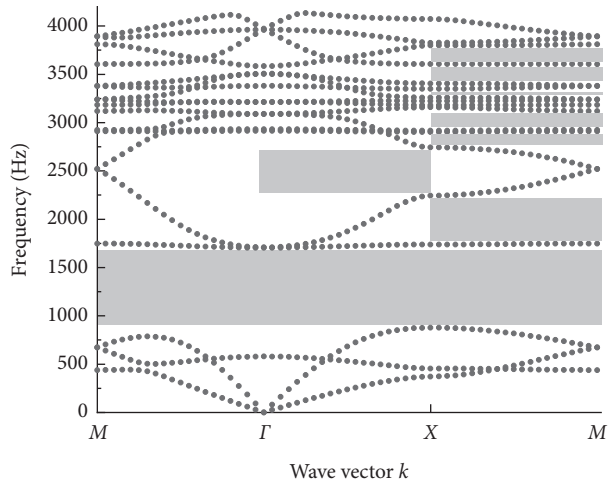

Figure 2: Band structure for xy-mode of damped rail with two-dimensional honeycomb PCs.

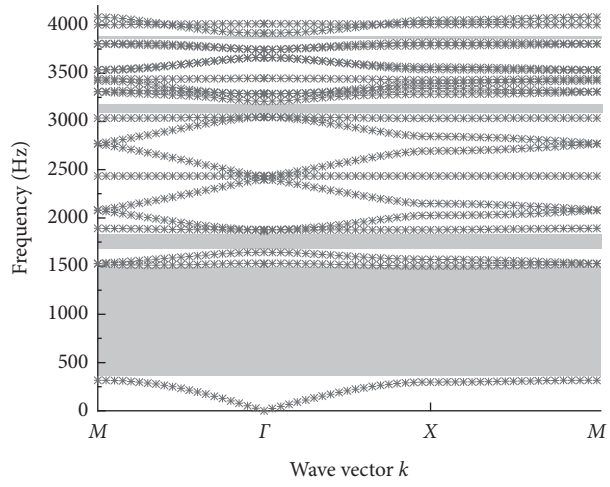

Figure 3: Band structure for (z)-mode of damped rail with two-dimensional honeycomb PCs.

structure, which are in the frequency ranges of 317.3~1501.7 Hz, 1645.3~1862.1 Hz, 3047.9~3208.2 Hz, and 3663.3~3740.6 Hz, respectively. The bandwidth decreases as the boundary frequencies increase. Within the above-mentioned band gaps, the propagation of shear waves in the proposed PCs structure will be inhibited.

Integrating the complete band gap for *xy*-mode and *z*-mode, it can be seen that there is an absolute band gap of the damped rail with two-dimensional honeycomb PCs in the frequency range of 877.3~1501.7 Hz, while the pinned-pinned resonant frequency of the rail (about 1000 Hz), which plays an important role in rail noise radiation and roughness growth [20], is also included in the band gap. It could be expected that the damped rail with PCs can suppress the pinned-pinned resonance of the rail effectively, which could improve the defect of traditional damped rails in the limited attenuation of pinned-pinned resonance of the rail [21].

2. Parametric Study

2.1. Effect of Filling Fraction. Taking the filling fraction as 0.40, 0.48, 0.52, 0.57, 0.61, 0.67, and 0.73, respectively, the boundary frequencies of the first complete band gaps for *xy*-mode and *z*-mode with different filling fractions are plotted in Figure 4. It can be observed that, with the decrease of the filling fraction, the boundary frequencies of the first complete band gaps for *xy*-mode and *z*-mode shift down and the influence on the ending frequency is more significant. Although a lower filling fraction is benefit for obtaining a band gap in lower frequency range, it will also bring a certain bandwidth loss. As the filling fraction varies from 0.73 to 0.40, the bandwidth of the absolute band gap (the shadow zone) declines from 2131.2 Hz to 449.0 Hz. In order to obtain an absolute band gap including the pinned-pinned resonant frequency of the rail and ensure a larger bandwidth, the filling fraction is suggested to be about 0.50.

2.2. Effect of Scatterer Density. Figure 5 shows the boundary frequencies of the first complete band gaps as the material of the scatterer is set to be Au, Pb, steel, and Al, respectively. It can be seen that the decrease of scatterer density can lead to the increase of the boundary frequencies of the first complete band gaps, which has the greatest influence on the starting frequency for *xy*-mode and the least effect on the ending frequency for *z*-mode. When the lead scatterer is replaced with aluminum, the bandwidth of the absolute band gap (the shadow zone) descends from 812.6 Hz to 116.1 Hz. The decrease of scatterer density leads to higher boundary frequencies and narrows the bandwidth. Therefore, the scatterer should be made of metals with heavy density to obtain a better vibration reduction effect.

2.3. Effect of Elastic Modulus of Matrix. Taking the elastic modulus of the matrix as 0.3~1.5 MPa, the boundary frequencies of the first complete band gaps for *xy*-mode and *z*-mode with different elastic modulus of the matrix are illustrated in Figure 6. It shows that increasing the elastic modulus of the matrix will enlarge the boundary frequencies of the first complete band gaps both for *xy*-mode and *z*-mode. As the elastic modulus of the matrix varies from 0.3 MPa to 1.5 MPa, the starting frequency of the absolute band gap (the shadow zone) increases from 679.6 Hz to 1519.6 Hz, and the ending frequency increases from 1163.0 Hz to 2600.2 Hz. Thus, reducing the elastic modulus of the matrix could obtain a lower band gap, while the bandwidth will become narrow. In order to make the absolute band gap include the pinned-pinned resonant frequency of the rail, it is suggested that the elastic modulus of the matrix should be not more than 0.6 MPa.

3. Vibration Reduction Property

To discuss the vibration reduction property of the damped rail with two-dimensional honeycomb PCs, a three-dimensional finite element model of a half-track is established. The track type is selected as the ordinary slab track used in subways, without any vibration reduction measures. The parameters of the track are shown in Table 2.

As the track system is on the symmetry of its center line, only half of the track system, including a rail and half of the track slab, is established. Symmetry constraints are set on the end faces and track slab center face of the model. Undersurface of the model is fixed on the ground with fixed constraint. A vertical harmonic excitation is applied to the rail head. In order to eliminate the interference of the reflected vibration wave from the end of the rail, the length of the model is set as 24 m, which is 40 times the fastener span length. Vibration finite models of the half-track, the standard rail, and the damped rail with honeycomb PCs are shown in Figure 7.

Figure 8 shows the vertical displacement admittances of the standard rail and the damped rail with PCs at the excitation point. It can be seen that there are two vibration peaks in the vertical displacement admittance curve of the standard rail. The first peak is at about 200 Hz, which is caused by the first vertical bending mode of the integral track; the second peak is at about 1100 Hz, which is caused by the pinned-pinned resonance of the rail. As the pinned-pinned resonance is a natural vibration property of the periodically supported structure and the damped rail with PCs does not provide a reaction force to the pinned-pinned resonance like a DVA does, so the pinned-pinned resonance still exists in the damped rail with PCs. However, with the band gap property, the peak amplitude of the pinned-pinned resonance decreases obviously. Besides, compression and shear of the rubber matrix dissipate more vibration energy, which effectively reduces the vibration amplitude of the rail.

The vibration transmission losses along the standard rail and the damped rail with PCs, calculated by equation (7) [22], are shown in Figure 9.

$$\Delta = \frac{20 \log_{10}\left(|u_0|/|u_i|\right)}{L}, \tag{7}$$

where u_0 is the vertical displacement of rail at the excitation point; u_i is the vertical displacement of rail at the response

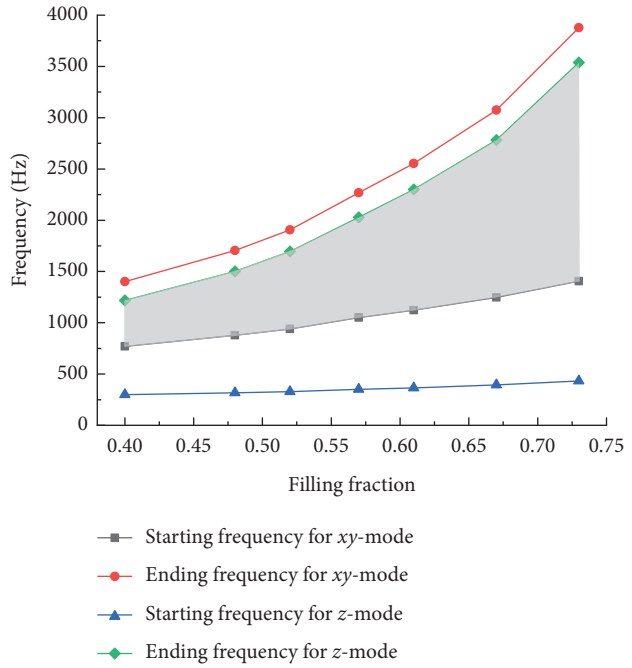

Figure 4: Effect of filling fraction on boundary frequencies of the 1st complete band gaps.

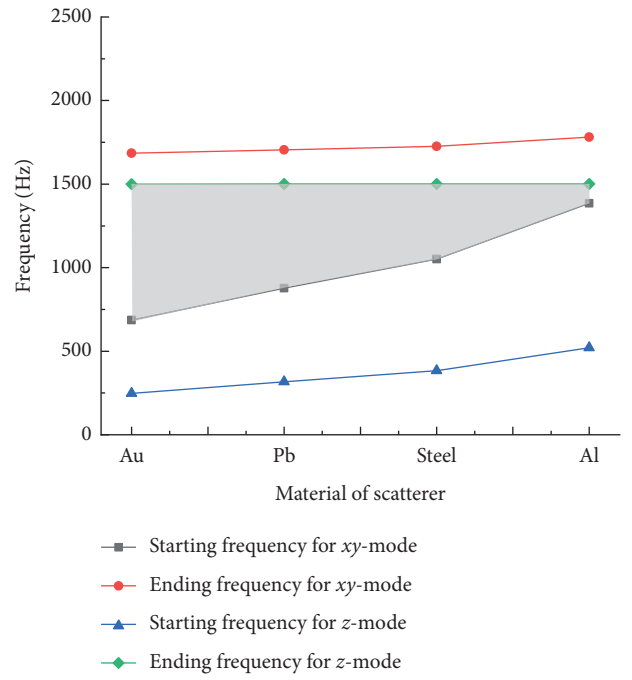

Figure 5: Effect of scatterer density on boundary frequencies of the 1st complete band gaps.

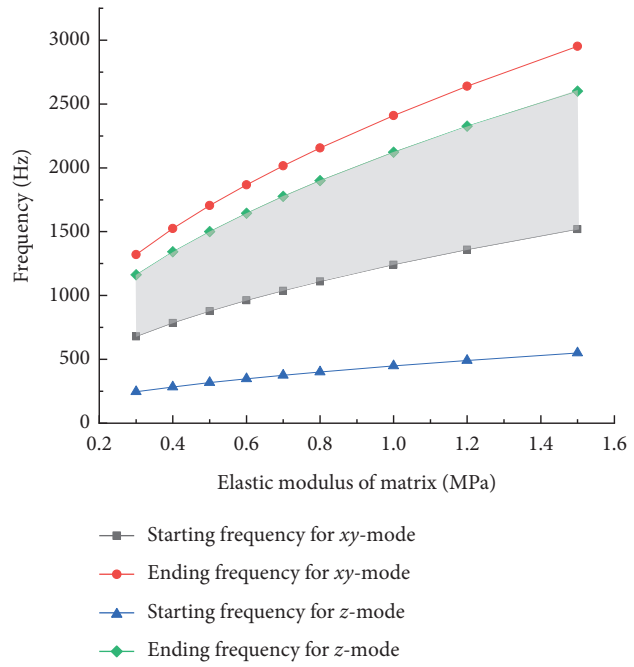

Figure 6: Effect of elastic modulus of matrix on boundary frequencies of the 1st complete band gaps.

Table 2: Material parameters of components in ordinary slab track.

Components	Material	Parameters	Values
Rail	60 kg/m	Density (kg/m^3)	7830
		Elastic modulus (Pa)	2.10×10^{11}
		Poisson's ratio	0.3
Short sleeper	C50	Density (kg/m^3)	2500
		Elastic modulus (Pa)	3.55×10^{10}
		Poisson's ratio	0.2
Bed	C35	Density (kg/m^3)	2500
		Elastic modulus (Pa)	3.30×10^{10}
		Poisson's ratio	0.2
Fastener	DTVI2 type	Vertical stiffness (N/m)	4.00×10^{7}
		Lateral stiffness (N/m)	1.00×10^{7}
		Vertical damping (N·s/m)	1.00×10^{4}
		Lateral damping (N·s/m)	0.20×10^{4}

point; and L is the distance between the excitation point and the response point. The point on the center of the rail head with five times the fastener span length from the excitation point is taken as the response point.

In Figure 9, it can be observed that the vibration transmission loss of the standard rail reaches the lowest

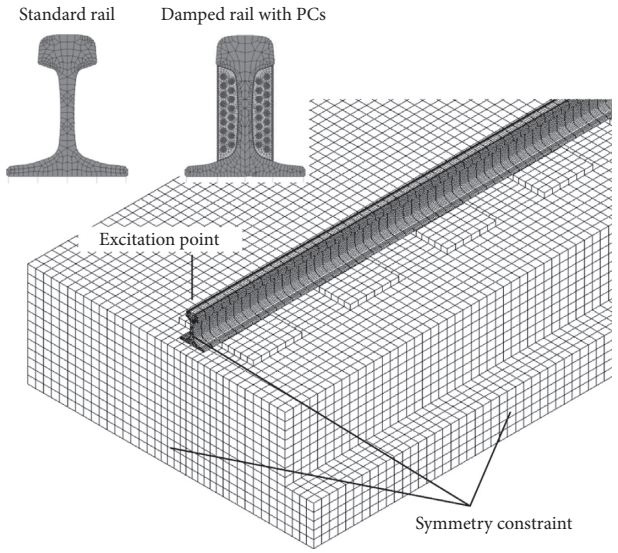

Figure 7: Vibration finite models of half-track, standard rail, and damped rail with honeycomb PCs.

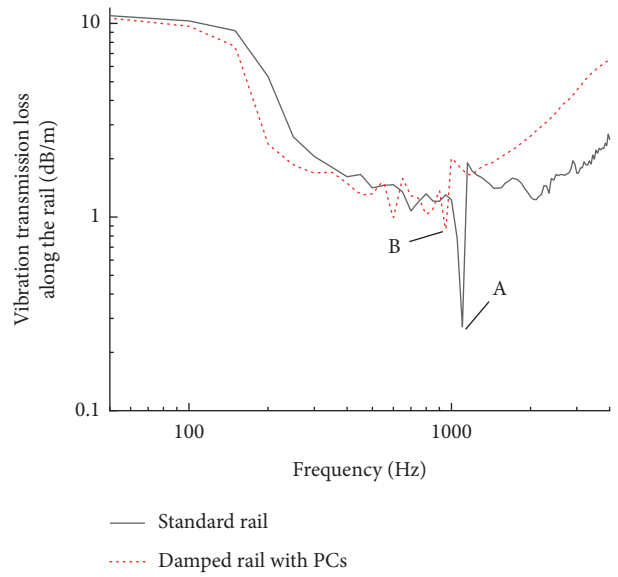

Figure 9: Vibration transmission losses of standard rail and damped rail with PCs.

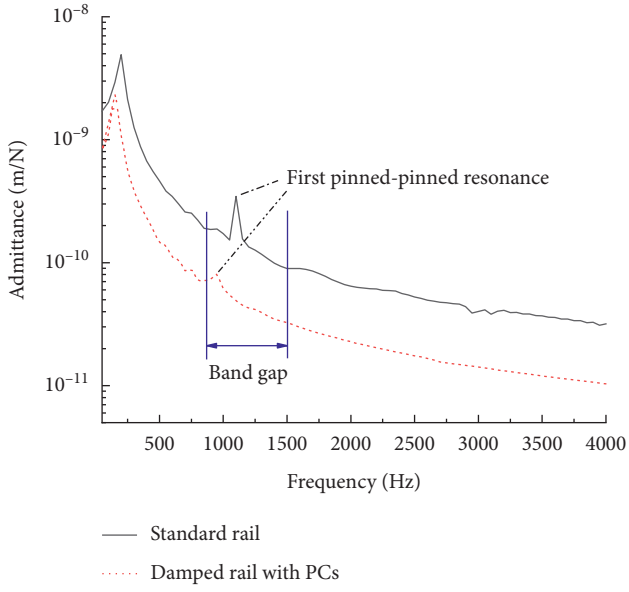

Figure 8: Vertical displacement admittances of standard rail and damped rail with PCs at excitation point.

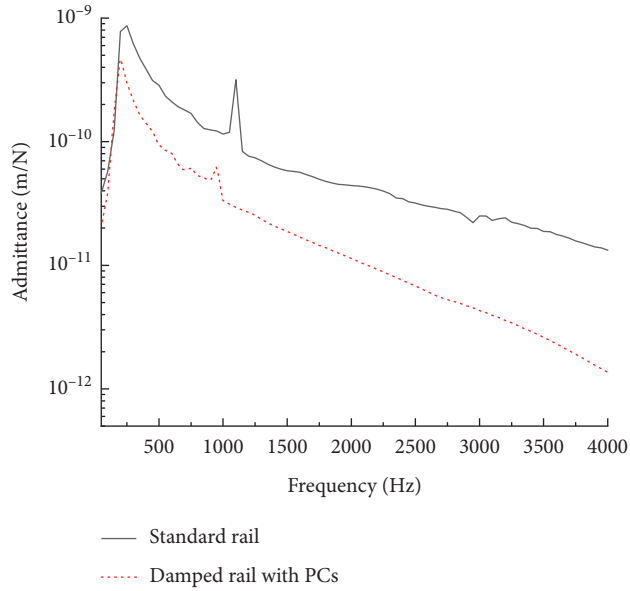

Figure 10: Vertical displacement admittances of standard rail and damped rail with PCs at response point.

point (point A in Figure 9) at the pinned-pinned resonant frequency, while it could be improved effectively by adding the damped rail with PCs (point B in Figure 9). Although vibration transmission loss of damped rail with PCs is lower than that of the standard rail in medium and low-frequency ranges, it can be seen from Figure 10 that the rail vibration at five times the fastener span length from the excitation point is still significantly reduced after using a damped rail with PCs, which shows that the damped rail with PCs has a good attenuation effect on the rail vibration.

4. Conclusions

In this paper, a damped rail with two-dimensional honeycomb PCs is proposed, and its band gap and vibration properties are studied. The following conclusions can be drawn from this work:

(1) The proposed damped rail with two-dimensional honeycomb PCs can generate an absolute band gap

in the frequency range of 877.3~1501.7 Hz, within which the propagation of compression wave or shear wave will be suppressed.

(2) Reducing the filling fraction and the elastic modulus of the matrix can obtain a band gap in a lower frequency range but also bring a narrower bandwidth. The decrease of the scatterer density will lead to higher boundary frequencies of the absolute band gap and descends the bandwidth. In order to obtain an absolute band gap which can suppress the pinned-pinned resonance of the rail and ensure a larger bandwidth, the filling fraction is suitable to be about 0.5, and the elastic modulus of the matrix is suggested to be not more than 0.6 MPa. Scatterer should be made of metals with heavy density to obtain a better vibration reduction effect.

(3) Through the comparison of vertical vibration displacement admittances and transmission losses of the standard rail and the damped rail with PCs, it could be seen that the proposed damped rail with PCs not only retains the advantage of dissipating energy through compression and shear of the rubber but also suppresses the vibration of pinned-pinned resonance of the rail with its band gap property. Thus, the damped rail with PCs presents a good performance in the attenuation of rail vibration, which provides a new approach to improve the vibration reduction performance and simplify the design process of damped rails.

Data Availability

The data used to support the findings of this study are available from the corresponding author upon request.

Conflicts of Interest

The authors declare that there are no conflicts of interest regarding the publication of this paper.

Acknowledgments

The research reported herein was supported by the National Natural Science Foundation of China (Grant no. 51805373).

References

[1] M. S. Kushwaha, P. Halevi, L. Dobrzynski, and B. Djafari-Rouhani, "Acoustic band structure of periodic elastic composites," *Physical Review Letters*, vol. 71, no. 13, pp. 2022–2025, 1993.

[2] X.-B. Xiao, Y.-G. Li, T.-S. Zhong, and X.-Z. Sheng, "Theoretical investigation into the effect of rail vibration dampers on the dynamical behaviour of a high-speed railway track," *Journal of Zhejiang University-Science A*, vol. 18, no. 8, pp. 631–647, 2017.

[3] P. Wang, Q. Yi, C.-Y. Zhao, M.-T. Xing, and J. Lu, "Wave propagation control in periodic track structure through local resonance mechanism," *Journal of Central South University*, vol. 25, no. 12, pp. 3062–3074, 2018.

[4] X. Sheng, C.-Y. Zhao, Q. Yi, P. Wang, and M.-T. Xing, "Engineered metabarrier as shield from longitudinal waves: band gap properties and optimization mechanisms," *Journal of Zhejiang University-Science A*, vol. 19, no. 9, pp. 663–675, 2018.

[5] X. Z. Nong, X. Li, T. H. Liu, X. Sheng, P. Wang, and C. Y. Zhao, "Band gap characteristics of vibration isolators of phononic crystals under floating slab," *Journal of Southwest Jiaotong University*, vol. 54, no. 6, pp. 1203–1209, 2019.

[6] C. Y. Zhao, X. Li, X. Sheng, D. Y. Liu, and P. Wang, "Test and analysis of vibration transfer characteristics of new rubber isolation pad," *Railway Standard Design*, vol. 64, no. 2, pp. 6–9, 2020.

[7] B. L. Jiang, W. N. Liu, M. Ma, X. J. Sun, and M. H. Li, "Application of periodic pile in vibration isolation of rail transit based on bloch-floquet theory," *Journal of the China Railway Society*, vol. 40, no. 3, pp. 146–152, 2018.

[8] L. C. Miao, C. Li, L. J. Lei, and X. D. Liang, "Vibration attenuation and application of composition materials of periodic structures," *Chinese Journal of Geotechnical Engineering*, vol. 42, no. 6, pp. 1139–1143, 2020.

[9] Q. Yi, Y. H. Wang, X. Gao, C. Y. Zhao, and P. Wang, "Band gap properties and noise reduction performances of periodic noise barriers in rail transit," *Journal of Central South University (Science and Technology)*, vol. 50, no. 5, pp. 1263–1270, 2019.

[10] R. X. Cui, L. Gao, X. P. Cai, and B. W. Hou, "Vibration and noise reduction properties of different damped rails in high-speed railway," *Noise Control Engineering Journal*, vol. 62, no. 4, pp. 176–185, 2014.

[11] A. C. Eringen and E. S. Suhubi, *Elastodynamics, Volume II: Linear Theory*, Academic Press, New York, NY, USA, 1975.

[12] M. S. Kushwaha, P. Halevi, G. Martínez, L. Dobrzynski, and B. Djafari-Rouhani, "Theory of acoustic band structure of periodic elastic composites," *Physical Review B*, vol. 49, no. 4, pp. 2313–2322, 1994.

[13] S. G. Zuo, X. J. Wei, and T. X. Ni, "The effects of viscoelastic material on the band gap of one-dimensional locally resonant phononic crystal," *Journal of Functional Materials*, vol. 47, no. 10, pp. 10162–10167, 2016.

[14] H. S. Shu, X. G. Wang, and R. Liu, "Bandgap analysis of cylindrical shells of generalized phononic crystals by transfer matrix method," *International Journal of Modern Physics B*, vol. 29, no. 24, Article ID 1550176, 2015.

[15] Q. Q. Wen, G. J. Yu, L. Y. Wang, and S. J. Zhu, "Band gap vibration isolation of phononic crystals based on magneto-rheological elastomers," *Journal of Synthetic Crystal*, vol. 47, no. 9, pp. 1843–1849, 2018.

[16] P. Xiang and X. D. Ding, "Sound attenuation by viscoelastic polymer containing hollow glass microspheres," *Journal of Ship Mechanics*, vol. 22, no. 7, pp. 908–914, 2018.

[17] X.-X. Su, J.-B. Li, and Y.-S. Wang, "A postprocessing method based on high-resolution spectral estimation for FDTD calculation of phononic band structures," *Physica B: Condensed Matter*, vol. 405, no. 10, pp. 2444–2449, 2010.

[18] D. J. Mead, "A general theory of harmonic wave propagation in linear periodic systems with multiple coupling," *Journal of Sound and Vibration*, vol. 27, no. 2, pp. 235–260, 1973.

[19] X.-F. Liu, Y.-F. Wang, Y.-S. Wang, and C. Zhang, "Wave propagation in a sandwich plate with a periodic composite core," *Journal of Sandwich Structures & Materials*, vol. 16, no. 3, pp. 319–338, 2014.

[20] D. J. Thompson, *Railway Noise and Vibration: Mechanisms, Modelling and Means of Control*, Elsevier, Oxford, UK, 2009.

[21] L. Gao, R. X. Cui, B. W. Hou, and H. Xiao, "Sensitivity analysis of influence parameters on resonance characteristics of ballastless track rail," *Journal of Hunan University (Natural Sciences)*, vol. 45, no. 3, pp. 115–121, 2018.

[22] H. P. Liu, *A study on modelling, prediction and its control of wheel/rail rolling noise in high speed railway*, Ph.D. thesis, Shanghai Jiaotong University, Shanghai, China, 2011.